Korean J Physiol Pharmacol 2020;24(4):329-338
https://doi.org/10.4196/kjpp.2020.24.4.329

KJPP

Original Article

Luteolin reduces fluid hypersecretion by inhibiting TMEM16A in interleukin-4 treated Calu-3 airway epithelial cells

Hyun Jong Kim[1,2,#], JooHan Woo[1,2,#], Yu-Ran Nam[2,#], Yohan Seo[3,4], Wan Namkung[3,4], Joo Hyun Nam[1,2,*], and Woo Kyung Kim[2,5,*]

[1]Department of Physiology, Dongguk University College of Medicine, Gyeongju 38066, [2]Channelopathy Research Center (CRC), Dongguk University College of Medicine, Goyang 10326, [3]College of Pharmacy, Yonsei Institute of Pharmaceutical Sciences, Yonsei University, Incheon 21983, [4]Department of Integrated OMICS for Biomedical Science, WCU Program of Graduate School, Yonsei University, Seoul 03722, [5]Department of Internal Medicine, Graduate School of Medicine, Dongguk University, Goyang 10326, Korea

ARTICLE INFO

Received March 3, 2020
Revised April 3, 2020
Accepted April 20, 2020

***Correspondence**
Joo Hyun Nam
E-mail: jhnam@dongguk.ac.kr
Woo Kyung Kim
E-mail: wk2kim@naver.com

Key Words
Airway hypersecretion
Allergic rhinitis
Anoctamin-1
Luteolin

#These authors contributed equally to this work.

ABSTRACT Rhinorrhea in allergic rhinitis (AR) is characterized by the secretion of electrolytes in the nasal discharge. The secretion of Cl^- and HCO_3^- is mainly regulated by cystic fibrosis transmembrane conductance regulator (CFTR) or *via* the calcium-activated Cl^- channel anoctamin-1 (ANO1) in nasal gland serous cells. Interleukin-4 (IL-4), which is crucial in the development of allergic inflammation, increases the expression and activity of ANO1 by stimulating histamine receptors. In this study, we investigated ANO1 as a potential therapeutic target for rhinorrhea in AR using an ANO1 inhibitor derived from a natural herb. Ethanolic extracts (30%) of *Spirodela polyrhiza* (SP_{EtOH}) and its five major flavonoids constituents were prepared. To elucidate whether the activity of human ANO1 (hANO1) was modulated by SP_{EtOH} and its chemical constituents, a patch clamp experiment was performed in hANO1-HEK293T cells. Luteolin, one of the major chemical constituents in SP_{EtOH}, significantly inhibited hANO1 activity in hANO1-HEK293T cells. Further, SP_{EtOH} and luteolin specifically inhibited the calcium-activated chloride current, but not CFTR current in human airway epithelial Calu-3 cells. Calu-3 cells were cultured to confluency on transwell inserts in the presence of IL-4 to measure the electrolyte transport by Ussing chamber. Luteolin also significantly inhibited the ATP-induced increase in electrolyte transport, which was increased in IL-4 sensitized Calu-3 cells. Our findings indicate that SP_{EtOH} and luteolin may be suitable candidates for the prevention and treatment of allergic rhinitis. SP_{EtOH}- and luteolin-mediated ANO1 regulation provides a basis for the development of novel approaches for the treatment of allergic rhinitis-induced rhinorrhea.

INTRODUCTION

Allergic rhinitis (AR) is defined as an allergic inflammation of the nasal mucosa. Approximately 10%–40% of the global population suffers from AR [1]. Although AR is an upper respiratory tract inflammatory disease, people with AR may also suffer from allergic reactions in the lower respiratory tract, which can result in the development of asthma. Moreover, increases in the levels of airborne allergens and air pollutants, which are caused by climate change and air pollution, have led to an increase in the number of patients with AR and asthma [2].

Currently, AR is treated using oral antihistamines, intranasal corticosteroids, and leukotriene receptor antagonists [1,3-5]. However, these drugs cause side effects, including drowsiness, prolonged QT interval, throat irritation, epistaxis, stinging, burning, and nasal dryness [4-6]. Allergen immunotherapy is cur-

This is an Open Access article distributed under the terms of the Creative Commons Attribution Non-Commercial License, which permits unrestricted non-commercial use, distribution, and reproduction in any medium, provided the original work is properly cited.
Copyright © Korean J Physiol Pharmacol, pISSN 1226-4512, eISSN 2093-3827

Author contributions: Study conception and design: J.H.N. and W.K.K. Conducting experiments, acquisition of data, data analysis, and interpretation of data: H.J.K., J.W., Y-R.N., and Y.S. Drafting of the manuscript: H.J.K., J.W., Y-R.N., and J.H.N. Critical review of manuscript: W.N. and W.K.K. Final approval of manuscript for submission: J.H.N. and W.K.K.

rently emerging as a new treatment for AR; however, it is not yet widely used because its clinical efficacy and safety have not been fully demonstrated [7]. For example, it has been associated with a potential risk of causing anaphylaxis. Therefore, the development of treatment strategies for AR that are safe and effective is needed.

The clinical signs and symptoms of AR include nasal congestion, sneezing, and rhinorrhea. Rhinorrhea, which is also known as nasal hypersecretion, is caused by the excessive secretion of mucin (inflammatory secretion) and liquid (water efflux) from the nasal submucosal glands (SMGs) [8,9]. It results in an uncontrollable liquid outpour from the nose and contributes to difficulty in breathing, which is uncomfortable and disturbs cognitive functions of patients [8,10,11]. The secretion of water and salts from the serous cells in nasal submucosal glands is mainly driven by the active secretion of Cl^- and HCO_3^-, which is stimulated by cyclic AMP or Ca^{2+} [9]. The accumulation of these anions on the apical side of the lumen results in a local increase in the osmolarity, thereby allowing water molecules to move from the basolateral side *via* the solvent drag effect [9].

In previous studies, it was reported that the secretion of Cl^- and HCO_3^- from the apical membranes of the submucosal gland serous cells is mainly regulated by the cystic fibrosis transmembrane conductance regulator (CFTR) channel. However, a recent study suggested that the calcium-activated Cl^- channel (CaCC) contributes more than CFTR to the secretion of Cl^- *via* cholinergic stimulation [9]. Moreover, the hypersecretion of fluid and mucus from the SMGs during AR also involves CaCC. It was recently reported that TMEM16A (ANO1), one of the major CaCCs, is expressed in nasal epithelial cells. Interleukin (IL)-4 and IL-13 induce goblet cell metaplasia and increase the expression of ANO1 [12-14]. In AR, increased ANO1 expression significantly increases mucin and fluid secretion via the release of histamine and the stimulation of protease-activated receptor 2 or cholinergic receptors [15-17]. ANO1 expression is significantly increased in patients with AR [17]. Moreover, IL-4 augments Cl^- and mucin secretion in primary cultured human nasal epithelial cells; however, this is suppressed by ANO1 inhibitors [17,18]. ANO1 mediates the hypersecretion of mucus, electrolytes, and water *via* the release of histamine, which is an important mediator of AR [9,17,19]. Therefore, ANO1 has potential as a unique therapeutic target for the management of AR. In addition, ANO1 channel inhibitors can potentially serve as dual-acting agents by treating mucin and fluid hypersecretion.

Spirodela polyrhiza (L.) Schleid. (SP) is widely used to relieve inflammation, urticaria, and symptoms of skin irritation, including pruritus, eczema, and rash [20,21]. According to a recent report, SP exerts a potential inhibitory effect on the calcium release-activated calcium channel, which is encoded by the *ORAI1* gene and is responsible for Th2 activation and mast cell degranulation [22-24]. In addition, formulations containing SP or its ethanolic extract have been shown to alleviate allergic inflammation and pruritus in mice with atopic dermatitis [21,25].

In this study, we aimed to: (i) investigate whether ANO1 is a suitable therapeutic target to inhibit nasal hypersecretion induced by allergic rhinitis; and (ii) determine whether substances that inhibit ANO1 and are found in natural extracts are potential therapeutic candidates. Herein, we report whether SP extract and its chemical constituents, in particular, luteolin, alleviate electrolyte secretion by inhibiting ANO1 activity in human airway epithelial cells.

METHODS

Cell culture

HEK293T (human embryonic kidney) cells (catalog no. CRL-3216) were obtained from American Type Culture Collection (ATCC, Manassas, VA, USA) and cultured in Dulbecco's modified Eagle's medium (DMEM; Welgene Inc., Gyeongsan, Korea) supplemented with 10% fetal bovine serum (FBS) (Welgene Inc.) and 1% penicillin/streptomycin (P/S) (Life Technologies, Carlsbad, CA, USA). Calu-3 cells were purchased from ATCC and cultured in minimum essential medium (Gibco, Grand Island, NY, USA) supplemented with 10% FBS and 1% P/S. All cells were cultured at 37°C in a humidified incubator. HEK293T cells were cultured under 10% CO_2 conditions, whereas Calu-3 cells were cultured in 5% CO_2 conditions.

Transient transfection

To measure the ANO1-mediated current, HEK293T cells were transfected with human ANO1 (hANO1) expression vector using TurboFect transfection reagents (Thermo Scientific, Waltham, MA, USA), according to the manufacturer's instructions. The ratio of green fluorescent protein (pEGFP-N1, Life Technologies) to hANO1 vector (10:1) was used to confirm the successful transfection of the cells. HEK293T cells were prepared the previous day in a 35-mm culture dish (Thermo Fisher Scientific). Then, 1.8 mg of hANO1 vector, 0.2 mg pEGFP, and 4 ml of TurboFect were added to 200 μl of DMEM (without FBS and P/S), followed by incubation at 25°C for 15 min. Lastly, 2 ml of complete medium (DMEM, 10% FBS, and 1% P/S) was added to the mixture and cultured with the prepared HEK293T cells for 24 h.

Electrophysiology

The ANO1-mediated current in the hANO1-transfected HEK293T cells and Calu-3 cells was measured using the patch clamp technique. The CFTR-mediated chloride current (I_{CFTR}) in the Calu-3 cells was also measured. The current was recorded using an Axopatch 200B amplifier (Molecular Devices, Sunnyvale, CA, USA) and a Digidata 1440A interface (Molecular Devices). Sampling was performed at 10 kHz with a low-pass filter

set at 5 kHz. pCLAMP 10.4 software (Molecular Devices) was used for the analysis. The recorded currents were analyzed using pCLAMP 10.4, GraphPad Prism 6 (GraphPad, La Jolla, CA, USA), and Origin 8 (MicroCal LLC, Northampton, MA, USA). The cells were transferred into a perfusion chamber with a glass bottom and allowed to settle for 5–10 min. Patch pipettes were pulled from borosilicate glass capillaries (World Precision Instruments, Inc., Sarasota, FL, USA) using a flaming/brown micropipette puller (p-1000; Sutter Instrument, Novato, CA, USA) and fire-polished to a pipette resistance of 2-7 MW (Narishige, East Meadow, NY, USA). The bath solution contained 140 mM Tris-Cl, 10 mM HEPES, 5 mM glucose, 1 mM $MgCl_2$, and 2 mM $CaCl_2$ (pH 7.4, Tris-base). The pipette solution for hANO1 comprised 140 mM *N*-methyl-D-glucosamine-Cl (NMDG-Cl), 10 mM ethylene glycol-bis(2-aminoethylether)-*N,N,N′,N′*-tetraacetic acid (EGTA), 7.85 mM $CaCl_2$, 1 mM $MgCl_2$, and 5 mM HEPES (pH 7.2, Tris-base). In order to activate ANO1, the intracellular calcium concentration was set at 600 nM and calculated using WEBMAXC (Stanford University, https://somapp.ucdmc.ucdavis.edu/pharmacology/bers/maxchelator/webmaxc/webmaxcS.htm). The pipette solution for CFTR contained 140 mM NMDG-Cl, 10 mM HEPES, 10 mM EGTA, 3.3 mM $CaCl_2$, and 1 mM $MgCl_2$ (pH 7.2, NMDG-base). The intracellular calcium concentration was set at 600 nM and calculated using WEBMAXC. To obtain the current/voltage relationship (I/V curve) in hANO1, we applied ramp-like pulses from –100 mV to +100 mV for 1 s every 20 s at a holding potential of –60 mV. The I_{CFTR} was determined at a holding potential of 0 mV. In the Calu-3 cells, step pulse was fixed at a potential of –60 mV. Voltage was increased by 20 mV from –100 mV to 100 mV. The pulse was maintained for 3 s during each voltage change.

Short-circuit current measurement

For short-circuit current measurement, Calu-3 cells were plated onto collagen precoated 12-mm permeable Snapwell inserts (Corning-Costar, Cambridge, MA, USA) in DMEM supplemented with 10% FBS and 1% P/S. For the IL-4 treatment experiments, Calu-3 cells were cultured in DMEM supplemented with 10% FBS, 1% P/S, and 10 ng/ml IL-4 (Peprotech, Rocky Hill, NJ, USA) for 24 h.

Snapwell inserts containing Calu-3 cells were mounted in Ussing chambers (Physiologic Instruments, San Diego, CA, USA). The basolateral and luminal side chamber was filled with HCO_3^--buffered solution. The HCO_3^--buffered solution was composed of 120 mM NaCl, 5 mM KCl, 1 mM $MgCl_2$, 1 mM $CaCl_2$, 10 mM D-glucose, 5 mM HEPES, and 25 mM $NaHCO_3$ (pH 7.4). The cells were allowed to stabilize for 20 min at 95% O_2/5% CO_2 conditions at 37°C. Subsequently, luteolin was added in the apical chamber, and ATP was added to the basolateral chamber to induce cytosolic calcium increase. Apical membrane currents were measured with an EVC4000 Multi-Channel V/I Clamp (World Precision Instruments, Sarasota, FL, USA) and recorded using PowerLab 4/35 (AD Instruments, Castle Hill, Australia). The sampling rate was 4 Hz. Data were collected and analyzed using Labchart Pro 7 software (AD Instruments).

Preparation of 30% ethanolic extract of SP (SP_{EtOH})

The dried whole aquatic parts of SP cultivated in South Korea were purchased from Kwangmyungdang Medicinal Herbs Co. (Ulsan, Korea). The dried plant (200 g) was cut into small pieces and macerated in 2 L of 30% ethanol. Extraction was performed under reflux for 3 h under heated conditions. The resulting extract was filtered using filter paper (no. 1 filter paper; Whatman plc, Maidstone, UK). The extract was evaporated to dryness under reduced pressure to obtain SP_{EtOH} at a yield of 9.3%. The extract was stored at –20°C until use.

Analysis of SP_{EtOH}

SP_{EtOH} and the relevant standard compounds were analyzed by high-performance liquid chromatography (HPLC) (1290 system; Agilent, Santa Clara, CA, USA) at the Korea Basic Science Institute (Seoul, Korea). Chromatographic separation of SP_{EtOH} (10 mg/ml) was performed on a Poroshell 120 SB-C18 column (3.0 × 100 mm, 2.7 μm; Agilent) at a detection wavelength of 340 nm. The mobile phase (A, 0.05% formic acid; B, 0.05% formic acid in acetonitrile) was set a flow rate of 0.5 ml/min and run in gradient mode as follows: 5%–10% B for 3 min, 10%–30% B for 2 min, 30%–40% B for 5 min, 40%–90% B for 2.5 min, and equilibration with 5% B, successively.

Statistical analysis

Statistical analyses were performed using GraphPad Prism 6.0 and Origin 8.0. All results are expressed as the mean ± standard error of mean. Data were analyzed using one-way analysis of variance (ANOVA) and Bonferroni's *post-hoc* test. In case of the isolated chemical compound experiments, data were analyzed using paired Student's t-test for comparisons between two groups (control *vs.* chemical treatment). p-values < 0.05 were considered statistically significant.

RESULTS

Effect of SP extract on human ANO1

To elucidate whether ANO1-mediated calcium-activated Cl^- current (I_{ANO1}) is inhibited by SP_{EtOH}, a whole-cell patch clamp experiment was performed using hANO1-overexpressing HEK293T ($HEKT_{ANO1}$) cells. Whole-cell configuration using a pipette solution containing 600 nM free Ca^{2+} generates outward rectifying

Cl^- currents, which is a typical biophysical property of ANO1 [26]. After I_{ANO1} reached a steady state, the bath solution was serially treated with 30, 100, and 300 μg/ml SP_{EtOH}. At the end of experiment, T16Ainh-A01, which is a potent small-molecule inhibitor of ANO1 [27], was applied to confirm its basal current. As shown in Fig. 1A and B, I_{ANO1} was effectively inhibited by SP_{EtOH} by about 34.13% ± 2.14%, 57.1% ± 3.34%, and 87.96% ± 1.02% at concentrations of 30, 100, and 300 μg/ml, respectively. The normalized data are summarized in Fig. 1C.

The chemical components of SP_{EtOH}

According to previous reports, the ethanolic extract of SP contains the following flavonoids: orientin, vitexin, luteolin 7-O-glucoside (Lu 7-G), apigenin 7-O-glucoside (Api 7-G), luteolin, and apigenin [20]. Chromatograms from the HPLC analysis of SP_{EtOH} showed five peaks eluting at 5.7 min (1), 5.91 min (2), 6.008 min (3), 6.334 min (4), and 7.915 min (5) (Fig. 2A). By comparing the chromatograms with those of six standard compounds obtained from previous studies conducted under the same HPLC conditions (Fig. 2B), we confirmed the presence of five of these flavonoids in SP_{EtOH}. Only apigenin was not detected in the extract (Fig. 2A). In addition, we estimated the concentrations of the compounds in 1 mg/ml SP_{EtOH} by comparing the peak areas with those of known amounts of analytical standard compounds (Table 1). We found that 1 mg/ml SP_{EtOH} contains 77.99 μg/mg (173 μM) orientin, 12.61 μg/mg (29.1 μM) vitexin, 46.87 μg/mg (104.5 μM) Lu 7-G, 3.94 μg/mg (9.12 μM) Api 7-G, and 1.027 μg/mg (3.58 μM) luteolin. The chemical structures of the five compounds are presented in Fig. 2C.

Effects of SP_{EtOH} constituents on I_{ANO1}

We also investigated whether the five aforementioned compounds inhibit I_{ANO1} in $HEKT_{ANO1}$ cells. Each compound was tested at a concentration of 100 μM. As shown in Fig. 3A, luteolin and Lu 7-G significantly inhibited I_{ANO1} by 62.14% ± 4.3% and 18.51% ± 5.93%, respectively. The other constituents inhibited I_{ANO1} by < 15% (orientin, 5.49% ± 10.21%; vitexin, 8.29% ± 3.47%; and Api 7-G, 15.48% ± 5.39%). We also identified the constituents that contribute to the inhibitory effect of SP_{EtOH} on ANO1. Although 1 mg/ml SP inhibited I_{ANO1} by > 90%, a mixture of all five components inhibited I_{ANO1} by only 20.1% ± 4.71%. The normalized I_{ANO1} data are presented in Fig. 3B.

Effects of SP_{EtOH} on calcium-activated and cyclic adenosine monophosphate (cAMP)-activated Cl^- currents in human airway epithelial cells (Calu-3)

Airway epithelial glands secrete Cl^- ions, which are responsible for the secretion of water and mucus. Cl^- efflux across the apical membrane occurs via the cAMP-activated Cl^- channel CFTR and the CaCC ANO1 [9]. Therefore, we investigated whether SP_{EtOH} inhibits the two Cl^- channels, or only CaCC in Calu-3 cells. Using the whole-cell patch clamp technique, we generated a CaCC current (I_{CaCC}) using a pipette solution containing 600 nM free Ca^{2+}, followed by serial treatment with 0.3, 1, and 3 mg/ml SP_{EtOH}. As shown in Fig. 4A, SP_{EtOH} inhibited I_{CaCC} by 36.9% ± 0.11%, 64.47%

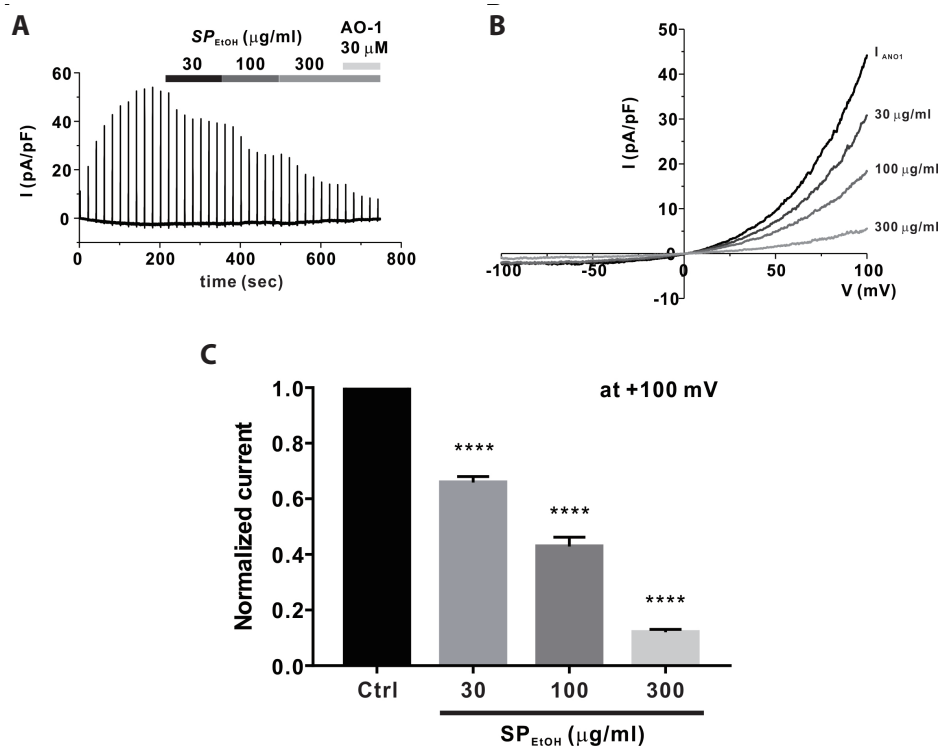

Fig. 1. Ethanolic (30%) extract of *Spirodela polyrhiza* (SP_{EtOH}) inhibits anoctamin-1 (ANO1)-mediated Cl^- current (I_{ANO1}) in ANO1-overexpressing HEK293T ($HEKT_{ANO1}$) cells. (A) Representative chart trace recordings showing the effects of 30, 100, and 300 μg/ml SP_{EtOH} on I_{ANO1}. At 300 μg/ml, SP_{EtOH} almost fully inhibited I_{ANO1}, similar to the effects of 30 μM T16Ainh-A01 (AO-1). (B) Typical current (I)/voltage (V) relationship curves for I_{ANO1}, showing the inhibition of I_{ANO1} by 30, 100, and 300 μg/ml SP_{EtOH}. (C) Summary of I_{ANO1} inhibition at +100 mV. Normalized amplitudes of currents (I_{Ext}/I_{ctrl} × 100%) were measured at a clamp voltage of +100 mV. Data are presented as the mean ± standard error of mean. Ext, SP_{EtOH}; ctrl, control. ****p < 0.0001 compared to the control (n = 6).

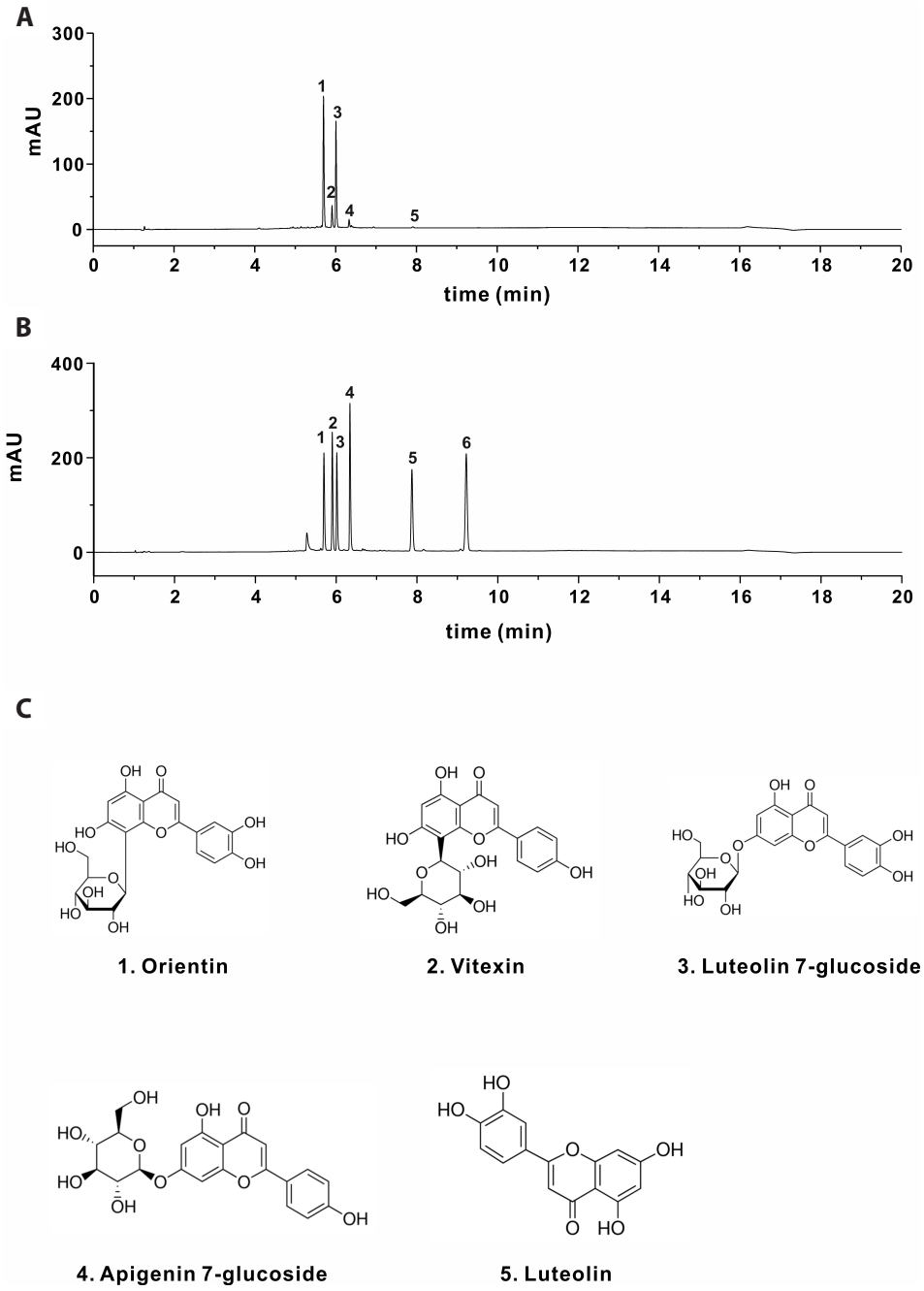

Fig. 2. High-performance liquid chromatography analysis of flavonoids in the ethanolic (30%) extract of *Spirodela polyrhiza* (SP_{EtOH}). (A) Five flavonoid compounds were found in SPEtOH and (B) identified as orientin (1), vitexin (2), luteolin 7-glucoside (3), apigenin 7-glucoside (4), luteolin (5), and apigenin (6). (C) The chemical structures of the identified compounds.

Table 1. Data obtained from high-performance liquid chromatography analysis of the five flavonoid compounds in the ethanolic (30%) extract of *Spirodela polyrhiza*

Compounds	RT (min)	Average area	Average amount (μg/ml)	Calculated amount[a] (μg/mg)
Orientin	5.7	329.2	7.799	77.992
Vitexin	5.91	56.1	1.261	12.605
Luteolin 7-glucoside	6.008	250.9	4.687	46.871
Apigenin 7-glucoside	6.334	19.7	0.394	3.944
Luteolin	7.915	5.1	0.103	1.027

RT, retention time. [a]Calculated amount = average amount × 50 (dilution factor)/5 mg.

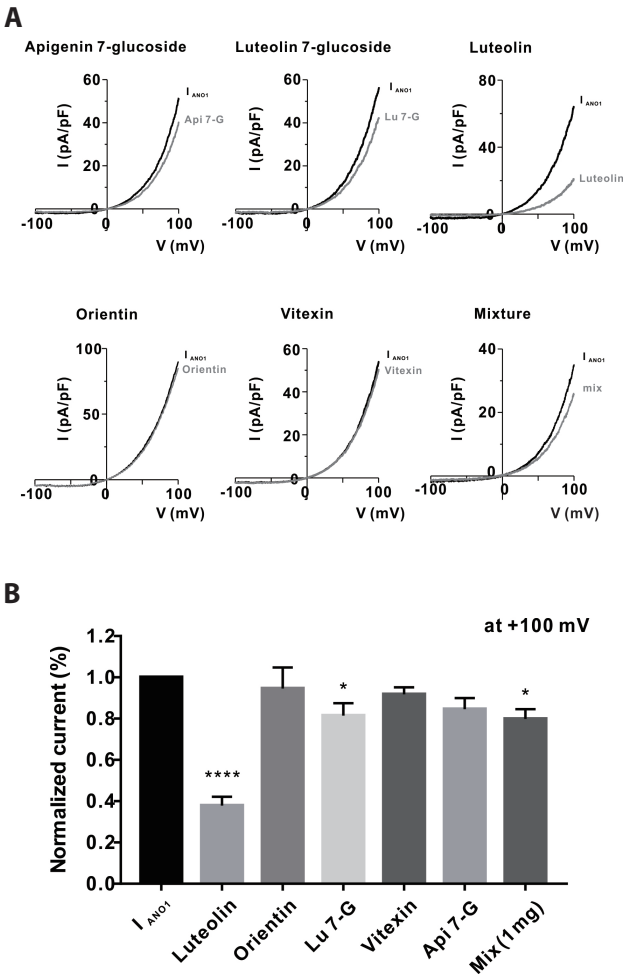

Fig. 3. Effects of orientin, vitexin, luteolin 7-glucoside (Lu 7-G), apigenin 7-glucoside (Api 7-G), and luteolin on anoctamin-1-mediated Cl^- current (I_{ANO1}). (A) Representative current (I)/voltage (V) relationship curves showing the effects of the five compounds on I_{ANO1}. Luteolin and Lu 7-G significantly inhibited I_{ANO1}. (B) Changes (%) in remaining current at +100 mV caused by the five identified compounds. Luteolin and Lu 7-G had a significant effect on I_{ANO1} at a concentration of 100 μM. ****p < 0.0001, *p < 0.05 compared to the control (n = 4).

± 0.04%, and 84.98% ± 0.04% at concentrations of 0.3, 1, and 3 mg/ml, respectively. Therefore, we investigated whether the activated current resulted from ANO1 expression by treating the cells with the ANO1-specific inhibitor 2-(4-chloro-2-methylphenoxy)-*N*-[(2-methoxyphenyl)methylideneamino]-acetamide (Ani9) (Fig. 4A). As a result, Ani9 was found to completely inhibit I_{CaCC}, which confirmed that I_{CaCC} resulted from ANO1 expression in Calu-3 cells. The normalized I_{CaCC} data are presented in Fig. 4B.

We observed that cAMP-activated Cl^- current (I_{CFTR}), which was mediated by CFTR, was not inhibited by SP_{EtOH} (Fig. 4C–E). Further, I_{CFTR} was induced by adding 10 μM forskolin, an adenylate cyclase activator, to the bath solution. We also confirmed the presence of I_{CFTR} by treating the cells with CFTRinh-172, which is a CFTR-specific inhibitor (Fig. 4C–E).

Luteolin inhibits I_{CaCC} in Calu-3 cells

Next, we investigated whether the five constituents of SP_{EtOH} modulate I_{CaCC} in Calu-3 cells. As observed in the $HEKT_{ANO1}$ cells, luteolin inhibited I_{CaCC} Sequential treatments with various concentrations of luteolin also resulted in the dose-dependent inhibition of I_{CaCC} (Fig. 5A). The half-maximal inhibitory concentration (IC_{50}) of luteolin against I_{CaCC} was found to be 27.91 ± 1.61 μM (Fig. 5B). However, the other flavonoids simply inhibited I_{CaCC} (Fig. 5C).

We tested the effect of a mixture of the five components at their respective concentrations in 1 mg/ml SP_{EtOH}; however, the mixture showed an inhibition rate of 37.02% ± 8.69%, which was half of the rate observed for 1 mg/ml SP_{EtOH}. Interestingly, luteolin showed different effects on I_{CFTR}. Treatment with 100 μM luteolin slightly potentiated I_{CFTR}, but significantly inhibited I_{CaCC} (Fig. 5D, E). Additionally, we confirmed the presence of I_{CFTR} by treating the cells with CFTRinh-172 (Fig. 5D, E). However, this phenomenon was only observed under a high concentration of luteolin (> 100 μM). Taken together, these results suggest that SP_{EtOH} and luteolin selectively inhibit ANO1 and may play critical roles in alleviating the hypersecretion of nasal mucus.

Luteolin suppresses electrolyte secretion in IL-4 treated Calu-3 cells

Since the patch clamp technique can only be used to measure the activity of ANO1, we performed Ussing chamber experiments to measure the total electrolyte transport across both ion channels and epithelial tissues. To this end, Calu-3 cells were cultured on transwell inserts to obtain an epithelial monolayer. The cells were then cultured with 10 ng/ml IL-4, which is one of the major cytokines causing allergic inflammation, for 24 days. Subsequently, the short-circuit currents (I_{SC}) of the treated cells were compared with those in case of the control cells. To evaluate the secretory function, calcium-dependent Cl^- secretion was stimulated by adenosine triphosphate (ATP). As expected, ATP treatment significantly increased I_{SC} in Calu-3 cells pretreated with IL-4 (Fig. 6A). As shown in Fig. 6B, treatment with luteolin significantly inhibited I_{SC} in a dose-dependent manner. Similar to the patch clamp experiments, the half-maximal inhibitory concentration (IC_{50}) of luteolin in Calu-3 cells was 23.13 ± 1.51 μM (Fig. 6C).

DISCUSSION

In the present study, we examined the inhibitory effect on ANO1 of SP_{EtOH}, which is reported to have a potential therapeutic effect on atopic dermatitis [21,25]. As a result, SP_{EtOH} was found to potently inhibit hANO1 channel activity in hANO1-overexpressing HEK293T cells by 87.96% ± 1.02% at a concentration of 300 μg/ml (Fig. 1). Furthermore, using HPLC, we found that orientin,

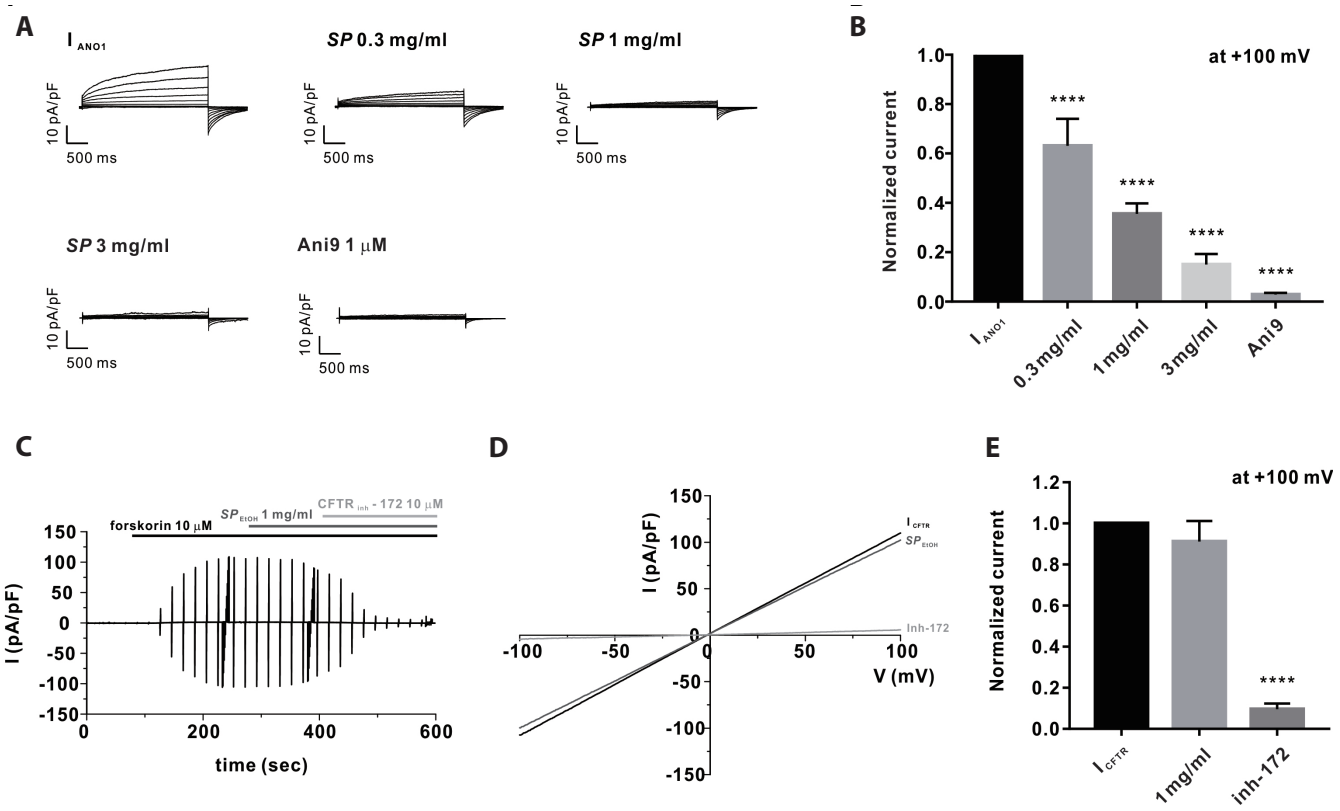

Fig. 4. Ethanolic (30%) extract of *Spirodela polyrhiza* (SP_{EtOH}) specifically inhibits the calcium-activated Cl^- current (I_{CaCC}) but not cystic fibrosis transmembrane conductance regulator (CFTR)-mediated Cl^- current (I_{CFTR}) in Calu-3 cells. (A) Representative traces of I_{CaCC} following activation by 600 nM intracellular free calcium and inhibition by SP_{EtOH} (0.3, 1, and 3 mg/ml) and 2-(4-chloro-2-methylphenoxy)-*N*-[(2-methoxyphenyl) methylideneamino]-acetamide (Ani9, 1 μM). The holding potential was –60 mV and 4-s step pulses (each 10 mV, –100 to +100 mV) were applied every second. (B) Bar graph showing normalized I_{CaCC} and its inhibition by SP_{EtOH}, which was calculated as $I_{Ext}/I_{ctrl} \times 100\%$ at +100 mV. Data are presented as the mean ± standard error of mean. ****$p < 0.0001$ compared to the control (n = 10). (C) A typical trace showing the amplitudes of I_{CFTR} and the effects of serially treating Calu-3 cells with 1 mg/ml SP_{EtOH} and 10 μM CFTRinh-172. The results show that I_{CFTR} was not modulated by SP_{EtOH}; however, it was completely inhibited by CFTRinh-172. (D) Representative current (I)/voltage (V) curves for I_{CFTR} after treatment with SP_{EtOH} and 10 μM CFTRinh-172. (E) Normalized current amplitude of I_{CFTR} at 100 mV. Data are presented as the mean ± SEM. ****$p < 0.0001$ compared to the control (n = 6).

vitexin, Lu 7-G, Api 7-G, and luteolin are the major flavonoids in SP_{EtOH} (Fig. 2) [20]. Based on the results of this quantitative analysis, we assessed whether these compounds were able to inhibit I_{ANO1} at individual concentrations of 100 μM or as a mixture. Luteolin and Lu 7-G inhibited I_{ANO1} by 62.14% ± 4.3% and 18.51% ± 5.93%, respectively (Fig. 3). The mixture of the constituents inhibited I_{ANO1} by only 20.1% ± 4.71%. This was much lower than the effect of SP_{EtOH}, which almost completely blocked I_{ANO1} at a concentration of 300 μg/ml. This was most likely due to the effect of other compounds in SP_{EtOH} besides the flavonoids.

Calu-3 cells have characteristics of human airway serous cells. They are widely used as a model of airway serous cells, which are involved in the secretion of electrolytes and water to hydrate airway surfaces [27-30]. Calu-3 cells express two representative Cl^- channels in airway epithelial cells: CaCC and CFTR. Therefore, experiments were conducted to determine whether SP_{EtOH} affects the activity of the two Cl^- channels. It was interesting to note that SP_{EtOH} inhibited I_{CaCC}, which was activated by increasing the intracellular calcium level (600 nM); however, it showed a lesser activity in the $HEKT_{ANO1}$ cells (64.47% ± 4.28% inhibition rate at a concentration of 1 mg/ml, Fig. 4). It was recently discovered that a novel potent small-molecule inhibitor, Ani9, completely inhibits I_{CaCC} [31]. Although this phenomenon has not been fully explained, it is presumed that differences in the distribution of regulatory proteins that interact with ANO1 or co-expression of ANO1 subtypes may be the underlying cause [28]. SP_{EtOH} did not have any effect on CFTR activity (Fig. 4), which confirmed that SP_{EtOH} only affects ANO1 activity. We then used Calu-3 cells to determine whether the flavonoid constituents in SP_{EtOH} can modulate I_{CaCC} and I_{CFTR}. The results showed that luteolin inhibits I_{CaCC} in Calu-3 cells to the same level as that in $HEKT_{ANO1}$ cells (IC_{50}, 27.91 ± 1.61 μM; Fig. 5). Recently, it has been reported that luteolin suppresses ANO1 activity in the human prostate cancer cell line PC-3 and $HEKT_{ANO1}$ cells, with an IC_{50} of about 9.5 μM [32,33], which indicates a higher sensitivity to these two cell types than to Calu-3 cells. This difference in IC_{50} values can be attributed to the differences in the cells. A similar observation was made for SP_{EtOH}, which showed different sensitivities to $HEKT_{ANO1}$ and

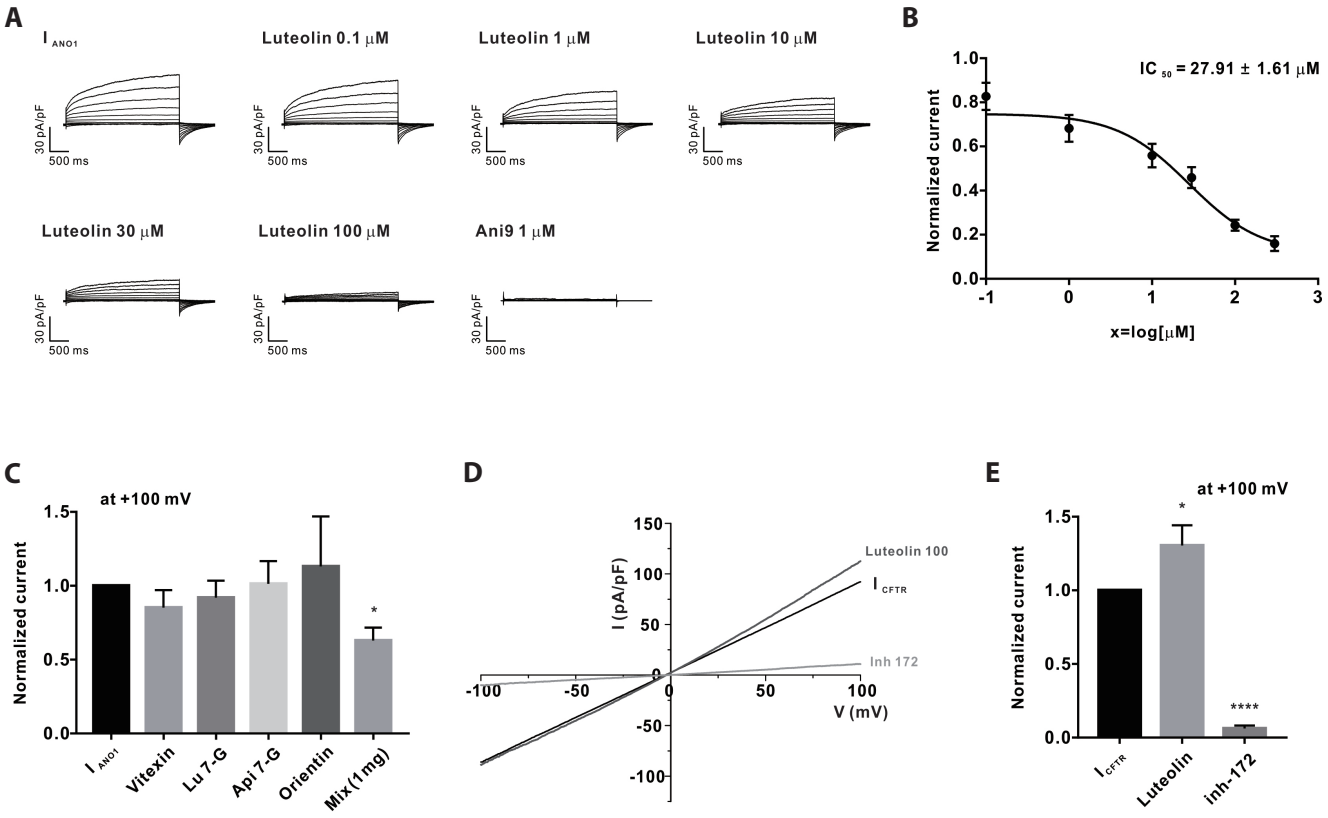

Fig. 5. Luteolin inhibits calcium-activated Cl^- channel current (I_{CaCC}), but slightly activates cystic fibrosis transmembrane conductance regulator (CFTR)-mediated Cl^- current (I_{CFTR}) at a high concentration (> 100 μM) in Calu-3 cells. (A) Representative traces of I_{CaCC}, obtained by applying step voltage pulses and inhibiting I_{CaCC} with various concentrations of luteolin and 2-(4-chloro-2-methylphenoxy)-*N*-[(2-methoxyphenyl) methylideneamino]-acetamide (Ani9). The holding potential was –60 mV and 4-s step pulses (each 10 mV, –100 to +100 mV) were applied every second. (B) Dose-response curve for luteolin-induced inhibition of I_{CaCC}. The half-maximal inhibitory concentration (IC_{50}) was 27.91 ± 1.61 μM. (C) Changes (%) in remaining current at +100 mV caused by vitexin, luteolin 7-glucoside (Lu 7-G), apigenin 7-glucoside (Api 7-G), orientin (each at a concentration of 100 μM), and a mixture of the five flavonoid compounds at their respective concentrations in the ethanolic (30%) extract of *Spirodela polyrhiza* (1 mg/ml). Data are presented as the mean ± standard error of mean. *p < 0.05 compared to the control (n = 4). (D) Representative current (I)/voltage (V) curve for I_{CFTR}. The curves show the effects of luteolin and CFTRinh-172 (inh-172) on I_{CFTR}. Luteolin slightly potentiated I_{CFTR} at a concentration of 100 μM. (E) Normalized current amplitude following the treatment of Calu-3 cells with 100 μM luteolin and inh-172. Data are presented as the mean ± SEM. *p < 0.05 compared to the control (n = 5).

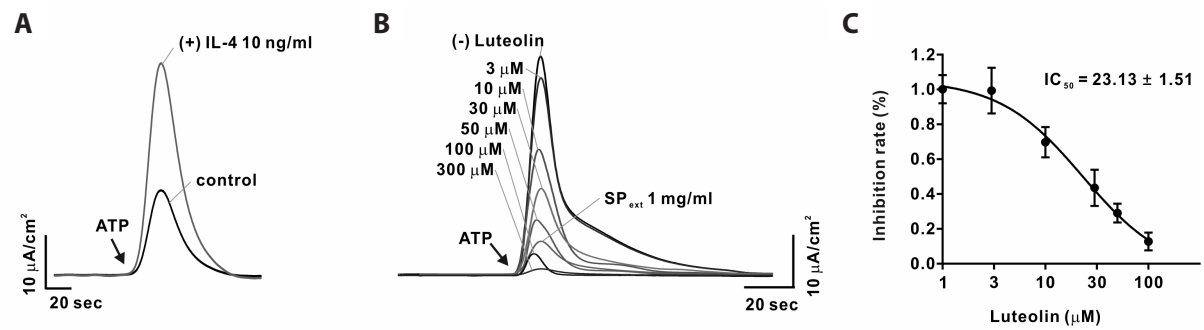

Fig. 6. Effects of luteolin on I_{SC} in interleukin-4 (IL-4)-treated Calu-3 cells. (A) Calu-3 cells were pretreated with IL-4 (10 ng/ml) for 24 h; CFTRinh172 was then added to the apical chamber and cells were incubated for 10 min prior to the treatment with adenosine triphosphate (ATP). Apical membrane currents were recorded for Calu-3 cells expressing anoctamin-1 (ANO1). (B) Representative current traces showing luteolin-mediated inhibition of ANO1 at the indicated concentrations. ANO1 was activated by 100 μM ATP. (C) Summary of dose-responses (mean ± standard error of mean, n = 4).

Calu-3 cells. It was also observed that luteolin only increased I_{CFTR} at high concentrations (> 100 μM).

Because Calu-3 cells form polarized monolayers when cultured on a transwell membrane filter [34], we performed Ussing chamber experiments on IL-4 (10 μg/ml)-treated Calu-3 cells to investigate the effect of luteolin on electrolyte transport through

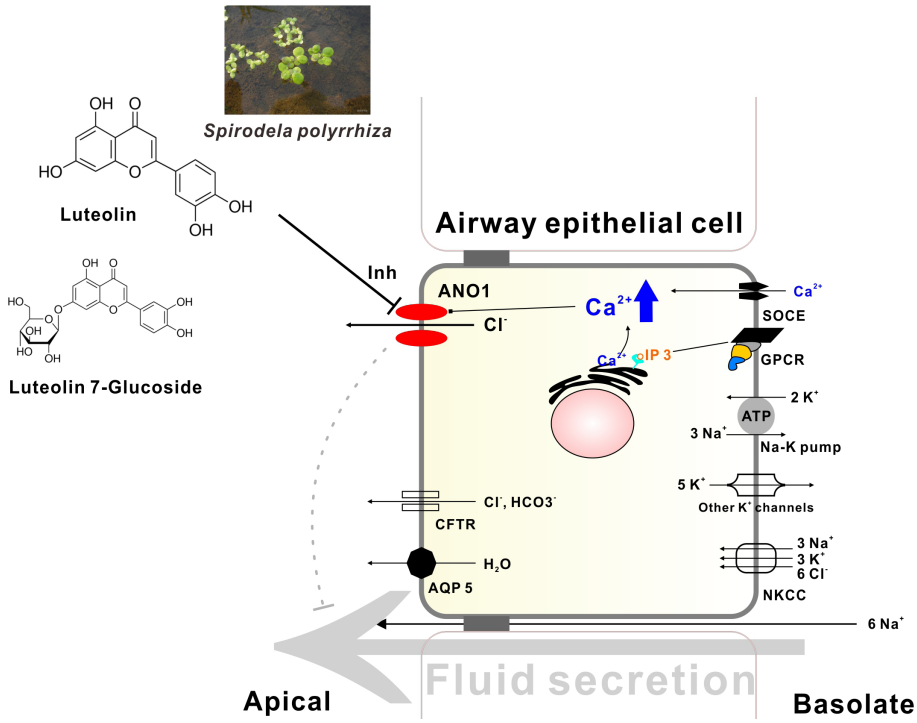

Fig. 7. Diagram illustrating the inhibitory effect of *Spirodela polyrhiza* (SP_{EtOH}) and its chemical constituents, luteolin and luteolin 7-glucoside, in electrolyte secretion *via* anoctamin-1 (ANO1) inhibition in the airway epithelium. CFTR, cystic fibrosis transmembrane conductance regulator.

the apical membrane. I_{SC} activated by purinergic receptor stimulation was strongly inhibited by luteolin treatment; the IC_{50} (27.91 ± 1.61 μM) was similar to that found for the ANO1 inhibition in the patch clamp study, indicating that luteolin inhibited the electrolytic secretion from the apical membrane by inhibiting ANO1 activity.

SP extract is used to treat allergic inflammatory diseases, such as atopic dermatitis. Furthermore, SP extract inhibits mast cell degranulation and suppresses IL-4 and IL-13 expression, which is mediated by Th2 cells [21,22,25]. Our study clearly showed that SP_{EtOH} and luteolin suppressed ANO1 activity, which is responsible for nasal hypersecretion in AR, in addition to alleviating electrolyte secretion via ANO1 inhibition in Calu-3 cells (Fig. 7). Therefore, our results demonstrated that ANO1 may serve as a potential therapeutic target for AR-induced rhinorrhea, whereby SP_{EtOH} and luteolin may be developed as agents for the prevention and treatment of AR. Moreover, our research can be used as a guide for the development of natural herbs as anti-allergic agents.

ACKNOWLEDGEMENTS

This research was supported by the Convergence of Conventional Medicine and Traditional Korean Medicine R&D program funded by the Ministry of Health & Welfare (Korea) through the Korean Health Industry Development Institute (KHIDI) (grant number HI16C0766) and also supported by the Basic Science Research Program through the National Research Foundation of Korea (NRF) funded by the Ministry of Education (NRF-2018R1A6A1A03023718).

CONFLICTS OF INTEREST

The authors declare no conflicts of interest.

REFERENCES

1. Brożek JL, Bousquet J, Agache I, Agarwal A, Bachert C, Bosnic-Anticevich S, Brignardello-Petersen R, Canonica GW, Casale T, Chavannes NH, Correia de Sousa J, Cruz AA, Cuello-Garcia CA, Demoly P, Dykewicz M, Etxeandia-Ikobaltzeta I, Florez ID, Fokkens W, Fonseca J, Hellings PW, *et al*. Allergic Rhinitis and its Impact on Asthma (ARIA) guidelines-2016 revision. *J Allergy Clin Immunol*. 2017;140:950-958.
2. D'Amato G, Pawankar R, Vitale C, Lanza M, Molino A, Stanziola A, Sanduzzi A, Vatrella A, D'Amato M. Climate change and air pollution: effects on respiratory allergy. *Allergy Asthma Immunol Res*. 2016;8:391-395.
3. Ricketti PA, Alandijani S, Lin CH, Casale TB. Investigational new drugs for allergic rhinitis. *Expert Opin Investig Drugs*. 2017;26:279-292.
4. Kakli HA, Riley TD. Allergic rhinitis. *Prim Care*. 2016;43:465-475.
5. Greiner AN, Meltzer EO. Pharmacologic rationale for treating aller-

gic and nonallergic rhinitis. *J Allergy Clin Immunol*. 2006;118:985-998.
6. Wheatley LM, Togias A. Clinical practice. Allergic rhinitis. *N Engl J Med*. 2015;372:456-463.
7. Dantzer JA, Wood RA. The use of omalizumab in allergen immunotherapy. *Clin Exp Allergy*. 2018;48:232-240.
8. Long R, Zhou Y, Huang J, Peng L, Meng L, Zhu S, Li J. Bencycloquidium bromide inhibits nasal hypersecretion in a rat model of allergic rhinitis. *Inflamm Res*. 2015;64:213-223.
9. Widdicombe JH, Wine JJ. Airway gland structure and function. *Physiol Rev*. 2015;95:1241-1319.
10. Rogers DF. Airway hypersecretion in allergic rhinitis and asthma: new pharmacotherapy. *Curr Allergy Asthma Rep*. 2003;3:238-248.
11. Kremer B, den Hartog HM, Jolles J. Relationship between allergic rhinitis, disturbed cognitive functions and psychological well-being. *Clin Exp Allergy*. 2002;32:1310-1315.
12. Galietta LJ, Pagesy P, Folli C, Caci E, Romio L, Costes B, Nicolis E, Cabrini G, Goossens M, Ravazzolo R, Zegarra-Moran O. IL-4 is a potent modulator of ion transport in the human bronchial epithelium *in vitro*. *J Immunol*. 2002;168:839-845.
13. Zhou Y, Shapiro M, Dong Q, Louahed J, Weiss C, Wan S, Chen Q, Dragwa C, Savio D, Huang M, Fuller C, Tomer Y, Nicolaides NC, McLane M, Levitt RC. A calcium-activated chloride channel blocker inhibits goblet cell metaplasia and mucus overproduction. *Novartis Found Symp*. 2002;248:150-165; discussion 165-170, 277-282.
14. Caputo A, Caci E, Ferrera L, Pedemonte N, Barsanti C, Sondo E, Pfeffer U, Ravazzolo R, Zegarra-Moran O, Galietta LJ. TMEM16A, a membrane protein associated with calcium-dependent chloride channel activity. *Science*. 2008;322:590-594.
15. Cho HJ, Choi JY, Yang YM, Hong JH, Kim CH, Gee HY, Lee HJ, Shin DM, Yoon JH. House dust mite extract activates apical Cl^- channels through protease-activated receptor 2 in human airway epithelia. *J Cell Biochem*. 2010;109:1254-1263.
16. Rievaj J, Davidson C, Nadeem A, Hollenberg M, Duszyk M, Vliagoftis H. Allergic sensitization enhances anion current responsiveness of murine trachea to PAR-2 activation. *Pflugers Arch*. 2012;463:497-509.
17. Kang JW, Lee YH, Kang MJ, Lee HJ, Oh R, Min HJ, Namkung W, Choi JY, Lee SN, Kim CH, Yoon JH, Cho HJ. Synergistic mucus secretion by histamine and IL-4 through TMEM16A in airway epithelium. *Am J Physiol Lung Cell Mol Physiol*. 2017;313:L466-L476.
18. Huang F, Zhang H, Wu M, Yang H, Kudo M, Peters CJ, Woodruff PG, Solberg OD, Donne ML, Huang X, Sheppard D, Fahy JV, Wolters PJ, Hogan BL, Finkbeiner WE, Li M, Jan YN, Jan LY, Rock JR. Calcium-activated chloride channel TMEM16A modulates mucin secretion and airway smooth muscle contraction. *Proc Natl Acad Sci U S A*. 2012;109:16354-16359.
19. Scudieri P, Caci E, Bruno S, Ferrera L, Schiavon M, Sondo E, Tomati V, Gianotti A, Zegarra-Moran O, Pedemonte N, Rea F, Ravazzolo R, Galietta LJ. Association of TMEM16A chloride channel overexpression with airway goblet cell metaplasia. *J Physiol*. 2012;590:6141-6455.
20. Qiao X, He WN, Xiang C, Han J, Wu LJ, Guo DA, Ye M. Qualitative and quantitative analyses of flavonoids in Spirodela polyrrhiza by high-performance liquid chromatography coupled with mass spectrometry. *Phytochem Anal*. 2011;22:475-483.
21. Lee HJ, Kim MH, Choi YY, Kim EH, Hong J, Kim K, Yang WM. Improvement of atopic dermatitis with topical application of Spirodela polyrhiza. *J Ethnopharmacol*. 2016;180:12-17.
22. Nam JH, Jung HW, Chin YW, Yang WM, Bae HS, Kim WK. Spirodela polyrhiza extract modulates the activation of atopic dermatitis-related ion channels, Orai1 and TRPV3, and inhibits mast cell degranulation. *Pharm Biol*. 2017;55:1324-1329.
23. Di Capite J, Parekh AB. CRAC channels and Ca^{2+} signaling in mast cells. *Immunol Rev*. 2009;231:45-58.
24. Kircher S, Merino-Wong M, Niemeyer BA, Alansary D. Profiling calcium signals of *in vitro* polarized human effector CD4+ T cells. *Biochim Biophys Acta Mol Cell Res*. 2018;1865:932-943.
25. Park BK, Park YC, Jung IC, Kim SH, Choi JJ, Do M, Kim SY, Jin M. Gamisasangja-tang suppresses pruritus and atopic skin inflammation in the NC/Nga murine model of atopic dermatitis. *J Ethnopharmacol*. 2015;165:54-60.
26. Yang YD, Cho H, Koo JY, Tak MH, Cho Y, Shim WS, Park SP, Lee J, Lee B, Kim BM, Raouf R, Shin YK, Oh U. TMEM16A confers receptor-activated calcium-dependent chloride conductance. *Nature*. 2008;455:1210-1215.
27. Namkung W, Phuan PW, Verkman AS. TMEM16A inhibitors reveal TMEM16A as a minor component of calcium-activated chloride channel conductance in airway and intestinal epithelial cells. *J Biol Chem*. 2011;286:2365-2374.
28. Kunzelmann K, Kongsuphol P, Aldehni F, Tian Y, Ousingsawat J, Warth R, Schreiber R. Bestrophin and TMEM16-Ca^{2+} activated Cl^- channels with different functions. *Cell Calcium*. 2009;46:233-241.
29. Fischer H, Illek B, Sachs L, Finkbeiner WE, Widdicombe JH. CFTR and calcium-activated chloride channels in primary cultures of human airway gland cells of serous or mucous phenotype. *Am J Physiol Lung Cell Mol Physiol*. 2010;299:L585-L594.
30. Banga A, Flaig S, Lewis S, Winfree S, Blazer-Yost BL. Epinephrine stimulation of anion secretion in the Calu-3 serous cell model. *Am J Physiol Lung Cell Mol Physiol*. 2014;306:L937-L946.
31. Seo Y, Lee HK, Park J, Jeon DK, Jo S, Jo M, Namkung W. Ani9, a novel potent small-molecule ANO1 inhibitor with negligible effect on ANO2. *PLoS One*. 2016;11:e0155771.
32. Seo Y, Ryu K, Park J, Jeon DK, Jo S, Lee HK, Namkung W. Inhibition of ANO1 by luteolin and its cytotoxicity in human prostate cancer PC-3 cells. *PLoS One*. 2017;12:e0174935.
33. Zhuo RG, Peng P, Zheng JQ, Zhang YL, Wen L, Wei XL, Ma XY. The glycine hinge of transmembrane segment 2 modulates the subcellular localization and gating properties in TREK channels. *Biochem Biophys Res Commun*. 2017;490:1125-1131.
34. Devor DC, Singh AK, Lambert LC, DeLuca A, Frizzell RA, Bridges RJ. Bicarbonate and chloride secretion in Calu-3 human airway epithelial cells. *J Gen Physiol*. 1999;113:743-760.